Hyperfine Interactions (2019) 240: 15
https://doi.org/10.1007/s10751-019-1554-2

Design and thermal modeling of a cold finger open cycle cryostat for Mössbauer spectroscopy

Natalia Andrea Gutiérrez Andrade [1] · Álvaro Andrés Velásquez Torres [1]

Published online: 18 February 2019

Abstract
In this work we present the design and thermal modeling of a cold finger open cycle cryostat that operates with liquid nitrogen, intended to be implemented into the Mössbauer spectrometer available at the Universidad EAFIT of Medellín, Colombia, with the purpose of obtaining a low cost and good performance system for the acquisition of low temperature Mössbauer spectra. Initially, we propose a design that meets the requirements of the spectrometer, afterward, based on the initial design, we develop the calculations of heat flow into the system. The results of the thermal model allowed us to define the dimensions of the vessels, as well as calculate the evaporation time of a given column of liquid nitrogen in the cryogenic vessel. Finally, some progresses in the construction of the physical prototype are presented.

Keywords Cryostat · Liquid nitrogen · Thermal modeling · Simulation · Mössbauer spectroscopy

1 Introduction

Cryogenics has been present in Mössbauer spectroscopy since the first Mössbauer spectra was obtained, by then Rudolf Mössbauer developed a cryostat to allow the recoilless resonance absorption in ^{191}Ir [1], by considering that the Debye-Waller factor gives a higher probability of having a zero phonon process as the temperature of the solid decreases [2]. In addition, cryogenics offers several advantages in Mössbauer spectroscopy, because in some materials containing Mössbauer nuclei, which exhibit paramagnetic or superparamagnetic behavior at room temperature, the reduction of temperature introduces magnetic ordered states in the structure [3], allowing measuring the magnetic hyperfine interaction in Mössbauer nuclei, as

Proceedings of the 16th Latin American Conference on the Applications of the Mössbauer Effect (LACAME 2018), 18-23 November 2018, Santiago de Chile, Chile

Electronic supplementary material The online version of this article (https://doi.org/10.1007/s10751-019-1554-2) contains supplementary material, which is available to authorized users.

✉ Álvaro Andrés Velásquez Torres
avelas26@eafit.edu.co; ngutie10@eafit.edu.co

[1] Grupo de Electromagnetismo Aplicado, Universidad EAFIT, A.A. 3300, Carrera 49 N° 7 Sur-50, Medellín, Colombia

well as a univocal assignment of phases in the sample. Structural changes can be also studied by lowering the temperature of the samples, among them the Verwey transition in magnetite [4].

Cryostats are devices that carry the sample to low and stable temperatures (below 160 K) by employing a heat sink, termed cryogen substance. These systems stabilize the temperature of the sample by isolating it from its surroundings and reducing the heat flows capable of reaching the heat sink. Commercial cryostats are expensive systems, being the cost of simpler configurations around USD 30,000. Although some designs of cryostats developed specifically for Mössbauer spectroscopy have been reported in literature [5, 6], more effort is necessary to develop a thermal model that allows to address an optimized design of this system, in order to minimize the thermal loads of the cryogenic substance, as well as obtaining Mössbauer spectra of good quality. The need to implement a low cost cryostat for the Mössbauer spectrometer of the Universidad EAFIT in Medellín, Colombia, motivated us to perform the design and construction of a prototype adapted to our particular requirements. In the next sections, we show the steps developed to design the cryostat and estimate its cryogenic performance.

2 Design of the cryostat

2.1 Conceptual design

The first step of the design process was to define a conceptual design of the cryostat according to the needs of the laboratory. The desired characteristics of the cryostat were delimited to be an open cycle system, based on evaporation of liquid nitrogen and holding the sample in a cold finger [7] to facilitate the transmission of 14.4 keV gamma rays through it. Based on these requirements, we analyzed the conceptual designs of commercial systems developed by the Janis Research Company [8]. Some of the most fitting designs are the ones presented in Fig. 1. These systems are composed of cylindrical vessels, where the inner vessel operates as the reservoir of the cryogen. The following vessel, termed radiation shield, is a double wall cavity that holds liquid nitrogen. This radiation shield is used specifically for liquid helium reservoirs or systems capable of reaching temperatures lower than 77 K, therefore it is not strictly necessary in our design. The outer structure is a vessel that operates as a vacuum jacket for the complete system. In these cryostats the sample is placed in a narrow extension of the outer vessel, termed tail, which can hold windows to facilitate the exposure of the sample to radiation.

As presented in Fig. 2, our design consists of two concentric cylindrical vessels, the inner vessel, termed cryogenic vessel, is made of stainless steel 304, which will operate as reservoir of liquid nitrogen, this vessel has the cold finger clamped at the bottom. The cold finger is made of copper OFHC (oxygen free high thermal conductivity copper). The outer vessel is made of aluminum 1100, which contains an aluminum cap at the bottom with a tail and two windows made of transparent acrylic of 3 mm thick and 5 cm diameter.

Initially, we made a search on available supplies that were closest possible to the dimensions reported in literature for cryostats used in Mössbauer spectroscopy, which were adaptable to the Mössbauer spectrometer developed at Universidad EAFIT [9]. According to this search, we selected the following dimensions for the cryogenic vessel: length: 0.8 m, internal radius: 0.038 m and wall thickness: 1.8 mm. These dimensions, in addition to adjusting to the proposed design, are available in commercial pipes of stainless steel 304. With the affordable dimensions, we proceeded to make the calculation of the heat flows towards a column of liquid

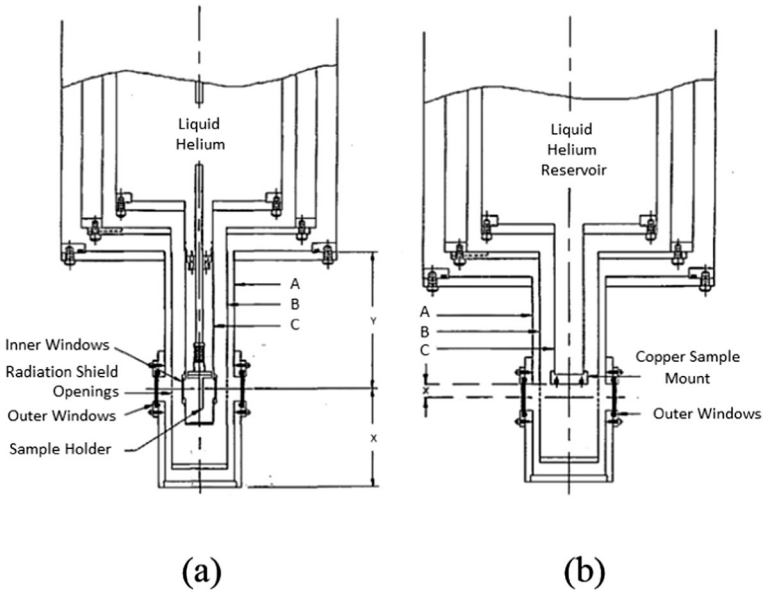

Fig. 1 Schemes of open cycle cryostats with tail and windows [8]. **a** Sample is immersed in the cryogen, **b** Sample is attached to a cold finger

nitrogen with a given height, in order to estimate the evaporation time of this column and determine if this is adequate for the acquisition of Mössbauer spectra.

The heat loads into the cryostat can be divided in two classes: variable loads, which change according to the level of liquid nitrogen in the cryogenic vessel, and constant loads like the heat flow by radiation coming from the cold finger and the bottom of the cryogenic vessel. Variable loads correspond to the conductive heat flow through the wall of the cryogenic vessel and the heat flow by radiation from the outer surface of the vessel. These heat loads were calculated for the different levels of liquid nitrogen and added to the constant heat flows.

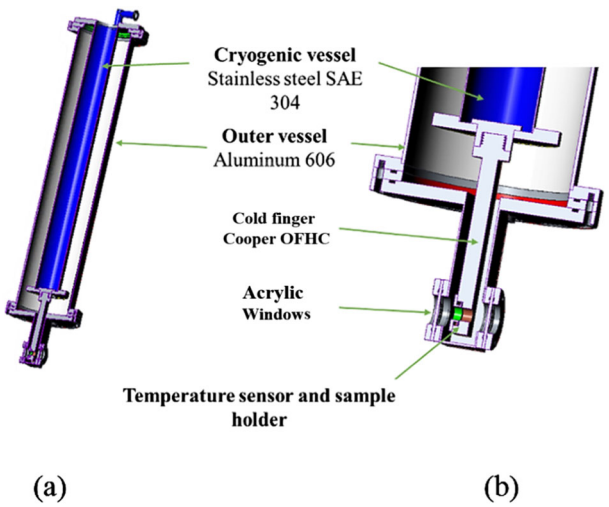

Fig. 2 Scheme of the proposed cryostat. **a** Internal view, **b** Detail of the cold finger and sample holder

Due to the non-analytical solution of the equations employed in the thermal model of the system, all calculations were performed numerically by programming scripts in the MATLAB software, version R2018b. The scripts programmed are reported as supplementary material of this work.

2.2 Heat flow by conduction

To calculate the heat flow by conduction into the cryogenic vessel, we applied the Fourier's law, as shown by [10]:

$$\dot{Q}_C = \frac{A}{L}\int_{T_1}^{T_2} K(T)dT \tag{1}$$

Where the calculated heat flow rate $\dot{Q}$ depends on the length L between the opening of the cryogenic vessel and the level of liquid nitrogen, and $K(T)$ is the thermal conductivity function, which depends on the temperature T at each point of the material; this function was taken from the NIST [11] and it was evaluated in the range between 297 K in the opening of the vessel and 77 K in the level of the liquid nitrogen. The function $K(T)$ was calculated numerically as follows:

$$\mathrm{K} = 10^{a} \tag{2}$$

Where,

$$\begin{aligned} a = {} & -1.4087 + 1.3982(\log_{10}T) + 0.2543(\log_{10}T)^2 - 0.6260(\log_{10}T)^3 \\ & + 0.2334(\log_{10}T)^4 + 0.4256(\log_{10}T)^5 - 0.4658(\log_{10}T)^6 \\ & + 0.165(\log_{10}T)^7 - 0.0199(\log_{10}T)^8 \end{aligned}$$

The variables considered in the model are schematized in Fig. 3a, while Fig. 3b shows the resulting heat flow by conduction as a function of the depth of the liquid nitrogen L, which variates from 0 to 0.8 m in steps of 1 cm. Figure 3b shows that the heat flow by conduction increases significantly with the decreasing of L, that is, while higher is the level of liquid nitrogen higher is the heat flow by conduction to the liquid nitrogen.

2.3 Heat flow by radiation

The heat flow by radiation was calculated using the radiation absorption equation for grey bodies in the geometry of coaxial cylinders, which is given by [12]:

$$\dot{Q}_{R\ e\to i} = \frac{\sigma A_{\mathrm{i}}\left({T_e}^4 - {T_{\mathrm{i}}}^4\right)}{\frac{1}{\varepsilon_i} + \frac{A_{\mathrm{i}}}{A_e}\left(\frac{1}{\varepsilon_e} - 1\right) + \frac{A_e}{A_i} - 1} \tag{3}$$

Where the subscript i denotes values that correspond to the inner vessel (cryogenic vessel), the subscript e denotes the properties of the outer vessel, $\sigma = 5.6704 \times 10^{-8}$ $\mathrm{WK^{-4}\ m^{-2}}$ is the Stefan Boltzman Constant, A refers to the lateral surface of the vessel, T is the temperature of

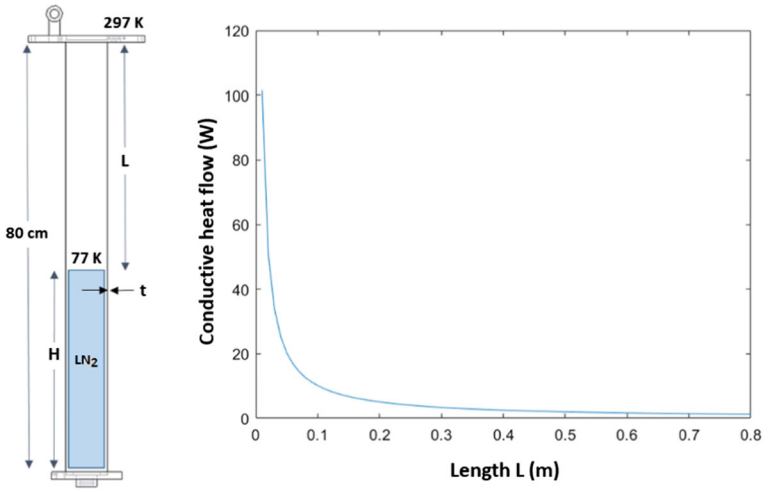

Fig. 3 **a** Variables of cryogenic vessel, L: length from the opening of the cryogenic vessel to the level of liquid nitrogen, H: height of the column of liquid nitrogen, t: wall thickness of the vessel, **b** Heat flow by conduction through a wall 1.8 mm thick in the cryogenic vessel with radius of 3.8 cm

the surface and ε is the emission coefficient of the material at temperature T, in this case $\varepsilon = 0.061$ for the stainless steel at 77 K, and $\varepsilon = 0.3$ for the aluminum alloy at 297 K [13]. In this approximation we considered two contributions for the heat flow by radiation, the first one is the radiation energy absorbed through the outer surface of the liquid nitrogen column; the second contribution corresponds to the radiation absorbed in the lateral surface of the conductive portion of the vessel, considering a linear temperature profile in this section, the surfaces of each contribution are shown in Fig. 4.

To calculate the main contribution of the heat flow by radiation, the Eq. (3) was calculated for each level of liquid nitrogen, therefore the independent variable is A_i, due to the relation of this value with the height of the column of liquid nitrogen. Then the contribution of the heat flow by radiation varies with L as presented in Fig. 5.

According to Fig. 5, the heat flow by radiation decreases as L increases, this is an expected behavior, because as observed in Fig. 3a, when the length L increases the lateral surface of the vessel surrounding the column of liquid nitrogen decreases.

The heat flow by radiation coming from the surface of the vessel placed above the liquid nitrogen depends on the temperature profile and the lateral surface area. This calculation was achieved by partitioning the lateral surface in small rings of equal area, placed at different altitudes, and then assigning to each ring a different value of temperature depending on its closeness to the opening of the vessel.

As all rings have the same area, the independent variable of the Eq. (3) in this calculation is the temperature T_i of i-th ring, then the heat flow was calculated for each ring and the heat flows of the different rings were added to obtain the total heat flow by radiation for each level of liquid nitrogen, which is presented in Fig. 6.

The addition of both contributions allows calculate the total heat flow by radiation to liquid nitrogen, which is presented in Fig. 7.

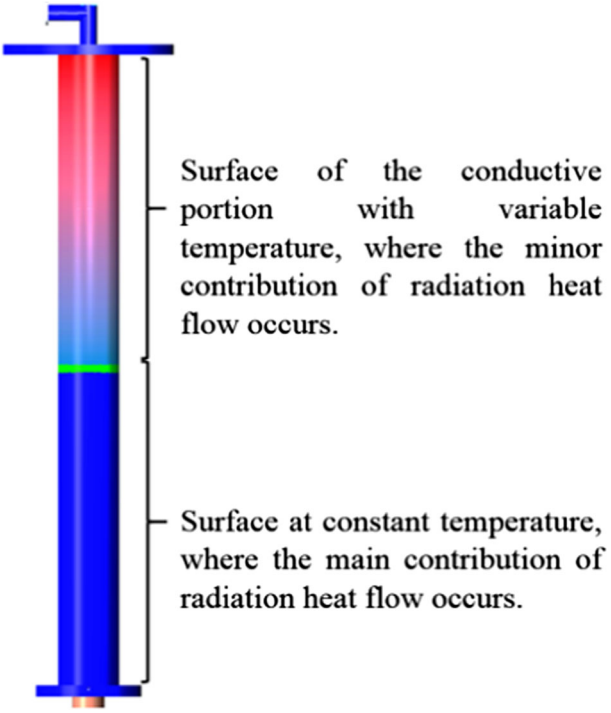

Fig. 4 Scheme of the cryogenic vessel, pointing the regions contributing to the heat flow by radiation to liquid nitrogen

The addition of heat flows by conduction and radiation gives us the total heat flow to the liquid nitrogen as a function of the length L from the opening of the cryogenic vessel to the surface of liquid nitrogen, which is presented in Fig. 8.

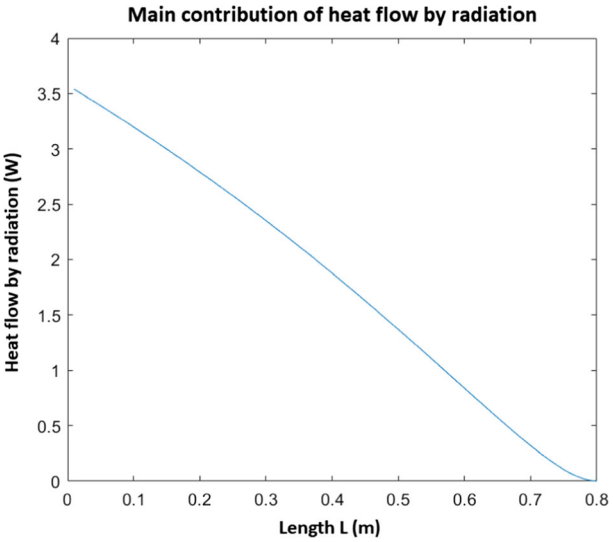

Fig. 5 Heat flow by radiation given in the surface of the cryogenic vessel surrounding the liquid nitrogen, as a function of length L between the opening of the cryogenic vessel and the level of liquid nitrogen

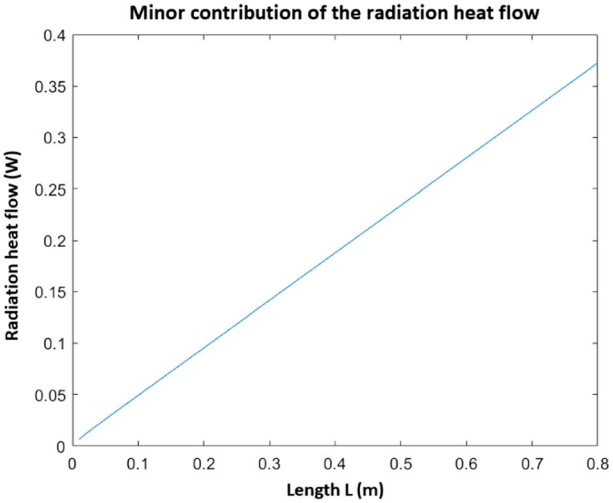

Fig. 6 Heat flow by radiation due to the surface of the cryogenic vessel above the liquid nitrogen, as a function of length L between the opening of the vessel and the level of liquid nitrogen

In addition to the variable heat flows, we have to consider constant heat loads due to heat flow by radiation coming from the bottom of the cryogenic vessel, the heat flow by radiation coming from the cold finger and the heat necessary to reduce the cold finger temperature from 297 K to 77 K. These heat loads, whose values are presented in Table 1, were calculated using the equation for heat flow by radiation in faced surfaces [12], which is presented in (4), considering the respective coefficients of the materials [13].

$$\dot{Q}_r = \frac{\sigma A\left(T_1{}^4 - T_2{}^4\right)}{\frac{1}{\varepsilon_1} + \frac{1}{\varepsilon_2}} \tag{4}$$

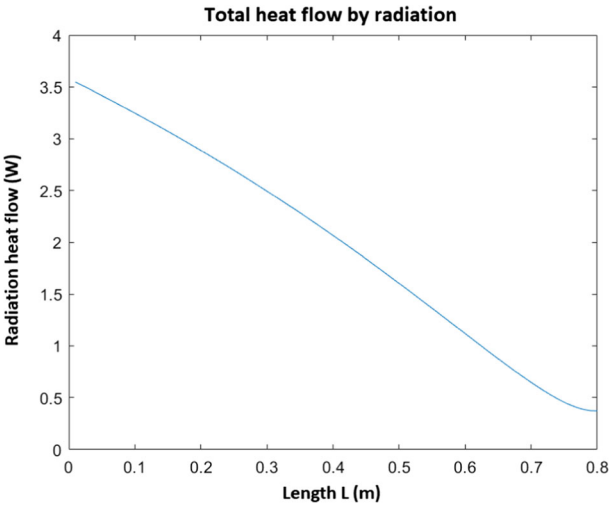

Fig. 7 Total heat flow by radiation as a function of the length L

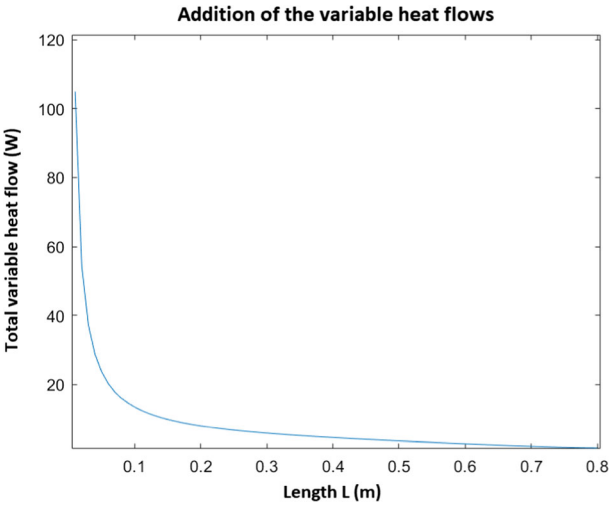

Fig. 8 Heat flow by conduction and radiation as a function of L

Where the subscript 1 indicates the values associated to the surface absorbing the radiation, and the subscript 2 indicates the values associated to the surface emitting the radiation. In this case only one value of area A is considered due to the similarity of area of the faced surfaces.

The heat extracted from the cold finger to reduce its temperature from 297 K to 77 K was calculated through the Black's law, using the coefficients for the specific heat of copper OFHC reported by the NIST [11].

2.4 Calculation of the evaporation time

To calculate the evaporation time t_e of a given column of liquid nitrogen, this column was partitioned in disks of 1 cm high, as presented in Fig. 9, afterward, the evaporation time was calculated as the sum of the evaporation times of the different disks that constitute the column, according to the equation:

$$t_e = \sum_{d=1}^{N} t_d \tag{5}$$

Where t_e is the evaporation time of the liquid nitrogen column for a specific level H, t_d is the individual time of evaporation of each disk, and N is number of disks in which the nitrogen column is divided.

Table 1 Constant heat loads in the cryostat

Heat load	Value
Heat flow by radiation coming from the bottom of the cryogenic vessel	2007 W
Heat flow by radiation coming from the cold finger	0,159 W
Heat extracted from the cold finger to bring it to 77 K	78×10^3 J

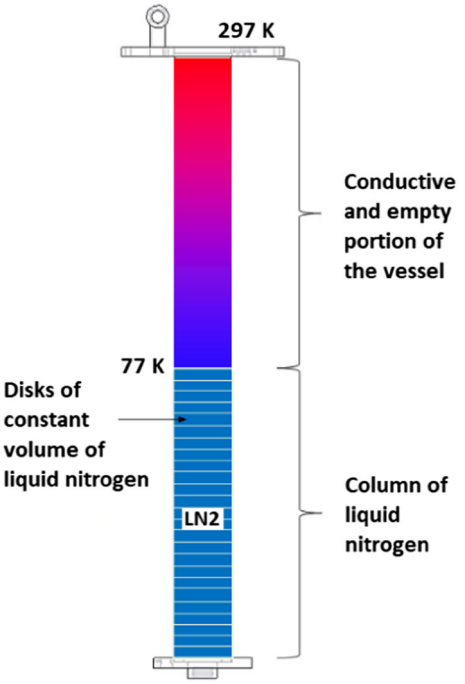

Fig. 9 Partition of the liquid nitrogen column in small disks, for estimating the evaporation time

The individual evaporation time of each disk of liquid nitrogen was calculated by dividing the evaporation heat required to evaporate the volume ΔV of the disk by the sum of variable heat flows and constant heat flows for the height of that specific disk, as presented in Eq. (6).

$$t_d = \frac{Q}{\dot{Q}_d} = \frac{\Delta V \times L_V}{\dot{Q}_{Cd} + \dot{Q}_{Rd} + \dot{Q}} \tag{6}$$

Where $L_V = 161.5$ J/mL is the latent evaporation heat of liquid nitrogen. By applying the Eq. (6) to each disk, we obtained the results presented in Fig. 10, where the evaporation time is measured as a function of the height of the disk within the liquid nitrogen column.

The total evaporation time of a column of liquid nitrogen is obtained by adding the individual times of evaporation of each disk. This is presented in Fig. 11 as a function of the level H of the liquid nitrogen.

Considering that the cold finger consumes 475 ml of liquid nitrogen to reduce its temperature from 297 K to 77 K, which is equivalent to 0.1 m of the column of liquid nitrogen, the evaporation time plot must be displaced 0.1 m to the right on the axis of liquid nitrogen level. Therefore, the evaporation time starts counting from the moment in which the thermal equilibrium between liquid nitrogen and cold finger is reached, as presented in Fig. 12.

With the design characteristics and calculations described before, the evaporation time of a column of liquid nitrogen of 0.8 m in length is 17.6 h. This is the maximum evaporation time, which applies when the cryogenic vessel is totally fill, containing a volume of 3.6 L of liquid nitrogen. This time is reasonable for programming refills of liquid nitrogen while the

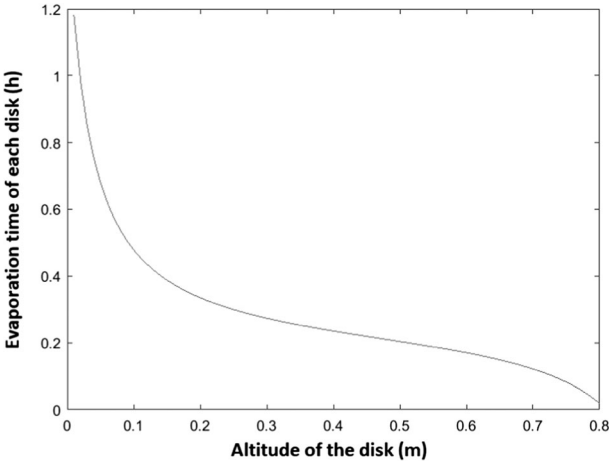

Fig. 10 Evaporation time of each disk as a function of its height within the liquid nitrogen column

acquisition of the Mössbauer spectrum of a sample takes place. Our thermal model predicts a mean evaporation rate of 0.2 L/h, this value is comparable with the rate 0.3 L/h reported by Frees and Fenger [5], in their design of a cold finger liquid nitrogen cryostat for Mössbauer spectroscopy.

3 Progress in the construction of the cryostat

After the design was defined, heat flows and evaporation time were calculated, we proceeded to the acquisition of the supplies required to build the cryostat. After mechanizing the components, we obtained the structure presented in Fig. 13.

Some internal components of the cryostat, as the cold finger and the cryogenic vessel are presented in Fig. 14.

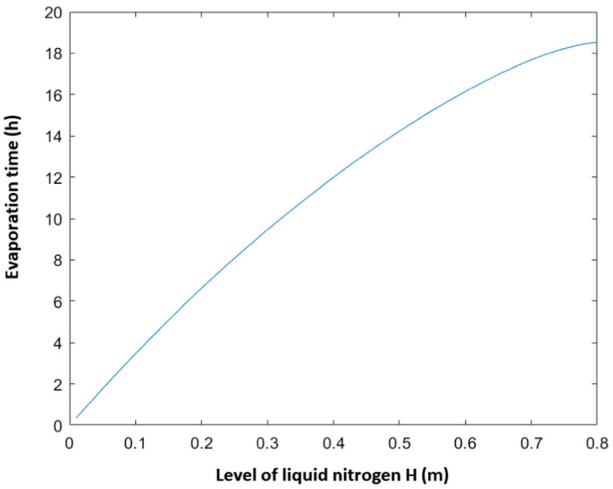

Fig. 11 Evaporation time of the liquid nitrogen column as a function of its height

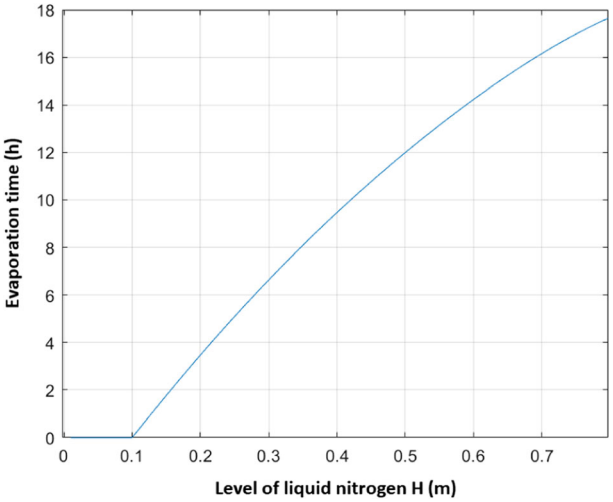

Fig. 12 Final calculated evaporation time of liquid nitrogen column as a function of its level

The system counts with two vacuum flanges, which follow the norm ISO KF 16. The vacuum O-ring seals implemented for the flanges between the vessels and the cap follow the norm AS 568. In addition to the vessels and the other materials, we developed a structure that

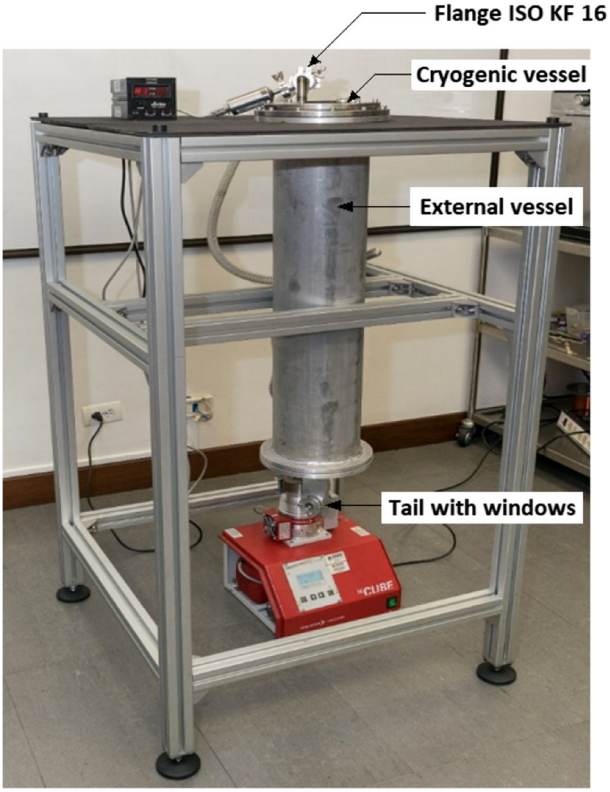

Fig. 13 Cryostat prototype built, placed in its support structure

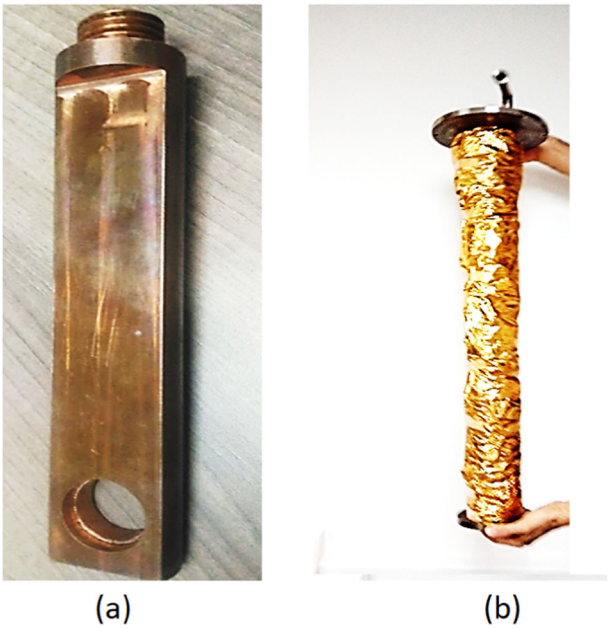

Fig. 14 Internal components of the cryostat. **a** Cold finger, **b** Cryogenic vessel

allows place the cryostat vertically in the Mössbauer spectrometer. For the sensing of temperature of the samples, we implemented a cryogenic temperature sensor, reference PT 111, supplied by Lake Shore. So far, the system is being tested to verify the conditions of vacuum necessary to satisfy the thermal isolation between the external and cryogenic vessels. As future work, we will measure experimentally the evaporation time for different lengths of column of liquid nitrogen, comparing the values obtained with those predicted by the model developed in this work. After corroborating the physical model of the cryostat, we will take Mössbauer spectra of known samples to validate the system for application in Mössbauer spectroscopy.

4 Conclusions

We have developed the design and thermal modeling of the heat flows into an open cycle cryostat of liquid nitrogen for Mössbauer spectroscopy. The proposed model allowed us to evaluate the design of the cryostat and selecting adequate dimensions for the needs of the system, according to commercially available supplies. The thermal model, based on conduction and radiation mechanisms, predicts an evaporation time of 17.6 h for a column of liquid nitrogen of 0.8 m, equivalent to 3.6 L. This time is reasonable for programming refills of liquid nitrogen during the acquisition of the Mössbauer spectrum of a sample. Some advances in the construction of the cryostat have been presented. As future work, we propose the validation of the thermal model with the physical prototype built, as well as the acquisition of Mössbauer spectra of known samples.

References

1. Mössbauer, R.L.: Kernresonanzfluoreszenz von Gammastrahlung in Ir191. Z. Phys. **151**, 124–143 (1958)
2. Eser, E., Askerov, I.M., Mamedov, B.A.: Calculation of the Debye–Waller factor of crystals using the n-dimensional Debye function involving binomial coefficients and incomplete gamma functions. Hyperfine Interact. **194**, 381–389 (2009)
3. van Lierop, J., Ryan, D.H.: Dynamics in fine particle magnets. Phys. Rev. B. (2002) https://doi.org/10.1103/PhysRevB.65.104402. Accessed 16 May 2018
4. Řezníček, R., Chlan, V., Štěpánková, H., Novák, P., Żukrowski, J., Kozłowski, A., Kąkol, Z., Tarnawski, Z., Honig, J.M.: Understanding the Mössbauer spectrum of magnetite below the Verwey transition: *Ab initio* calculations, simulation, and experiment. Phys. Rev. B. **96**(195124), (2017)
5. Frees, L.A., Fenger, J.: A simple mössbauer cryostat based on the "Cold-Finger" Principle. Danish atomic energy commission, research establishment riso, chemistry department (1973). http://orbit.dtu.dk/files/55857816/ris_m_1662.pdf. Accessed 14 June 2018
6. Novak, P., Pechousek, J., Malina, O., Navarik, J., Machala, L.: Liquid nitrogen cryostat for the low-temperature Mössbauer spectra measurements. AIP Conf. Proc. **1622**, 67–71 (2014)
7. Balshaw, N.H.: Practical cryogenics. Oxford instruments superconductivity limited. In: Witney (1996)
8. Jirmanus, M.N.: Introduction to laboratory cryogenics. Janis Research Company Inc. (1990)
9. Velásquez, A.A., Arroyave, M.: Implementation of a preamplifier-amplifier system for radiation detectors used in Mössbauer spectroscopy. Hyperfine Interact. **224**, 65–72 (2014)
10. Lebrun, Ph.:An introduction to cryogenics. CERN, Geneva (2007)
11. Marquardt, E.D., Le, J.P., Radebaugh, R.: Cryogenic material properties database. 11th international Cryocooler Conf. In: Proc (2000)
12. Levensipel, O.: Engineering flow and heat exchange. Plenum Press, pp. 161–165 and 178–183. New York (1993)
13. White, G.K.: Experimental techniques at low temperatures. Clarendon Press, Oxford (1979)